Chaos

Dynamics of multilayer networks with amplification

Cite as: Chaos **30**, 123136 (2020); https://doi.org/10.1063/5.0025529
Submitted: 16 August 2020 . Accepted: 01 December 2020 . Published Online: 17 December 2020

Thierry Njougouo, Victor Camargo, Patrick Louodop, Fernando Fagundes Ferreira, Pierre K. Talla, and Hilda A. Cerdeira

Dynamics of multilayer networks with amplification

Cite as: Chaos **30**, 123136 (2020); doi: 10.1063/5.0025529
Submitted: 16 August 2020 · Accepted: 1 December 2020 ·
Published Online: 17 December 2020

Thierry Njougouo,[1] Victor Camargo,[2,3] Patrick Louodop,[1] Fernando Fagundes Ferreira,[2,3] Pierre K. Talla,[4] and Hilda A. Cerdeira[5,a)]

AFFILIATIONS

[1]Research Unit Condensed Matter, Electronics and Signal Processing, University of Dschang, P.O. Box 67, Dschang, Cameroon
[2]Center for Interdisciplinary Research on Complex Systems, University of Sao Paulo, Av. Arlindo Bettio 1000, 03828-000 São Paulo, Brazil
[3]Department of Physics-FFCLRP, University of São Paulo, Ribeirao Preto, SP 14040-901, Brazil
[4]L2MSP, University of Dschang, P.O. Box 67, Dschang, Cameroon
[5]São Paulo State University (UNESP), Instituto de Física Teórica, Rua Dr. Bento Teobaldo Ferraz 271, Bloco II, Barra Funda, 01140-070 São Paulo, Brazil

[a)]**Author to whom correspondence should be addressed:** hilda.cerdeira@unesp.br

ABSTRACT

We study the dynamics of a multilayer network of chaotic oscillators subject to amplification. Previous studies have proven that multilayer networks present phenomena such as synchronization, cluster, and chimera states. Here, we consider a network with two layers of Rössler chaotic oscillators as well as applications to multilayer networks of the chaotic jerk and Liénard oscillators. Intra-layer coupling is considered to be all to all in the case of Rössler oscillators, a ring for jerk oscillators and global mean field coupling in the case of Liénard, inter-layer coupling is unidirectional in all these three cases. The second layer has an amplification coefficient. An in-depth study on the case of a network of Rössler oscillators using a master stability function and order parameter leads to several phenomena such as complete synchronization, generalized, cluster, and phase synchronization with amplification. For the case of Rössler oscillators, we note that there are also certain values of coupling parameters and amplification where the synchronization does not exist or the synchronization can exist but without amplification. Using other systems with different topologies, we obtain some interesting results such as chimera state with amplification, cluster state with amplification, and complete synchronization with amplification.

The research on multilayer networks has attracted a lot of attention in recent years in many areas of physics, engineering, social sciences, etc.[1–6] Some emergent behaviors in such systems due to interaction among the dynamical units reveal a variety of interesting phenomena, such as synchronization,[1,7,8] cluster formation,[9] explosive synchronization,[10] explosive desynchronization,[11] chimera,[12–16] etc. Among these, synchronization and chimeras are the most widely studied. The notion of amplification is very important in science and technology. This work presents an investigation of different phenomena such as complete synchronization, cluster formation, phase synchronization, and chimera states in a network with amplification. For an extended study, we present three cases with three different topologies.

I. INTRODUCTION

The structure of many real-world problems in nature, engineering, science, and technology is defined as a set of entities interacting with each other in complicated patterns that can produce multiple types of relationships that change in time and exhibits a plethora of emergent patterns or behaviors as synchronization, chimeras, chaos, consensus, cooperation, to mention a few. One very important ingredient behind most of those phenomena is the way in which the particles or agents forming the systems interact, i.e., the topology of the underlying network.

The network theory is used as an important tool for the modeling of dynamical processes in complex systems.[1,2,7] It also plays a major role in the investigation of collective behavior. It finds many applications in epidemiology where it is used to investigate epidemic

spreading, in the industry where it is used in the control of behavior of machines, in dynamics of populations with the control of the displacement of the individuals, the cars, the drones, or the airplanes. According to the these applications, we can mention that the main objective is the controllability of the network to lead to a certain state (it can be synchronization, cluster state, phase-flip, chimera state, etc.).[8,13,14,17–19] Thus, the investigation of the dynamics of the networks needs the expertise of some mathematical tools such as the Master Stability Function (MSF) developed by Pecora and Carroll, the transversal Lyapunov exponent, the correlation between the oscillators of the same and of a different layer, etc. One of the best methods to study the stability of the synchronization in the network is the master stability function.[20] This method is used for coupled identical oscillators.

Many researchers are studying several phenomena that take place in multiplex networks. Such an interest is motivated in understanding how the complete or partial synchronization occurs in this type of systems and also because the topologies of multiplex networks appear in several natural and technological systems. The multiplex network may be described as being a collection of two or more coupled networks where a set of networks is connected by links where the interactions are of different types.[21,22] These links characterize the connections existing between any node and the network of the multiplex network. Many recent works addressing multilayer structures and systems were summarized in Ref. 23.

The study of inter-layer synchronization in non-identical multilayer networks was addressed in Ref. 24. The authors were able to show an analytical treatment for a two-layer multiplex using the master stability function method. One interesting outcome was to predict the effect that missing links in one of the layers has on the inter-layer synchronization. Later, in Ref. 25, it was found that a sparse inhomogeneous second layer can promote chimera states in a sparse homogeneous first layer. The study of synchronization of non-identical multilayers is very recent, thus, many collective behavior properties and patterns may unravel.

Here, we consider a network with two layers where we choose an all-to-all coupling in the layer for the case of Rössler oscillators, a ring with bidirectional coupling in each layer for the case of jerk oscillators and a global mean field coupling for the last case mentioned above. The connection between the systems of both layers (interlayer coupling) is unidirectional. The main goal of this work is to investigate in each case the dynamics of each layer as well as the whole network with amplification in the second layer. We found the key values of the parameters to control synchronization with and without amplification.

The remainder of this work is organized as follows. In Sec. II, we present our multilayer network with the mathematical description of the model and the systems. The dynamics of the main case is presented in Sec. III, emphasizing on the intralayer and interlayer coupling in which numerical simulations are done. An application to another two systems has been studied in Sec. IV, and finally, we present the conclusions in Sec. V.

II. MULTILAYER NETWORK

The model consists of a multilayer network constituted of N nodes connected in each layer, which can be represented by a

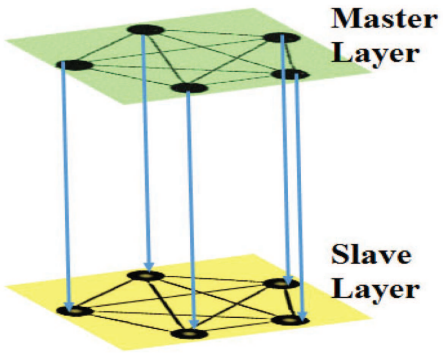

FIG. 1. Schematic representation of a network with two layers of interaction.

$2N \times 2N$ adjacency matrix A_{ij}, where the elements of this matrix are, respectively, 1 if the nodes i and j are connected and 0 if not. Based on Ref. 25, the adjacency matrix of the whole network consisting of two layers can be expressed as follows:

$$\mathbf{A} = \begin{pmatrix} A^1 & 0 \\ I & A^2 \end{pmatrix}, \tag{1}$$

where A^1 and A^2 are the $N \times N$ adjacency matrix modeling the intralayer connectivity in the first and second layer, respectively. I is an $N \times N$ identity matrix representing the unidirectional interactions (Layer 1 $\rightarrow$ Layer 2) between the oscillators with the same index in both layers. The use of the null matrix is justified by the non-existence of a connection from the slave layer to the master layer.

In the following, we consider a model of the multilayer network constituted of N nodes in each layer connected using an all-to-all coupling scheme in each layer (see Fig. 1). To each node corresponds a nonlinear autonomous Rössler oscillator as described in Ref. 26. Notice that it is this combined oscillator, which defines our network as a two-layer system made up of a driving system and a slave one.

The dynamics of the first layer also considered as the driver for the network is described by Eq. (2), where ϵ_1 is the intra-layer coupling strength for the first layer,

$$\begin{cases} \dot{x}_i^1 = -x_i^2 - x_i^3 + \epsilon_1 \sum_{k=1}^{N} A_{ik}^1 (x_k^1 - x_i^1), \\ \dot{x}_i^2 = x_i^1 + a x_i^2, \\ \dot{x}_i^3 = b x_i^1 + x_i^3 (x_i^1 - c). \end{cases} \tag{2}$$

The second layer has exactly the same intra-layer topology with similar systems in the nodes. The choice of systems in the second layer follows Louodop *et al.*[27] where the authors show in Appendix A that this form of coupling between elements of different layers produces generalized synchronization.[27] Notice that it is this system defined in Louodop *et al.*[27] what defines which oscillators in layer 2 interact with those in layer 1, while keeping the same all-to-all intralayer topology. Therefore, the dynamics of the second or slave layer

is given by Eq. (3),

$$\begin{cases} \dot{y}_j^1 = -y_j^2 - y_j^3 + \epsilon_2 \sum_{k=1}^{N} A_{jk}^2 (y_k^1 - y_j^1) + C_0 (x_j^1 - C_2 y_j^1), \\ \dot{y}_j^2 = \dfrac{x_j^1 + a x_j^2}{C_2}, \\ \dot{y}_j^3 = b y_j^1 + \dfrac{x_j^3 x_j^1}{C_2} - c y_j^3. \end{cases} \tag{3}$$

Here, ϵ_2 is the intra-layer coupling strength and C_0 is the interlayer coupling strength. It is important to mention that this inter-layer coupling exists only between the oscillators with the same index (i.e., for $i = j$, where the j index runs from 1 to N). C_2 is the parameter of proportionality named the amplification coefficient. This term or interaction via a *conjugate* variable has been used in the literature to model *revival*[28,29] as well as *amplitude death*.[30] For all these layers, we consider $a = 0.36$, $b = 0.4$, and $c = 4.5$, and we note that at these values of the parameters, the systems operate in the chaotic regime.[26] This topology of connectivity between the master and slave layers imposes generalized synchronization between both layers in the absence of intralayer coupling because as it is conceived (see Appendix A), the slave layer is supposed to function as an observer of the master layer with certain conditions $C_2 \neq 0$. In this work, we were interested in the notion of synchronization with amplification (or reduction) depending on the value of C_2. For $C_2 > 1$, we have amplification of the systems of the master layer (or a reduction of the systems of the slave layer) and conversely for $C_2 < 1$. It should be noted that when C_2 takes negative values there is an anti-synchronization between the systems of the master layer and those of the slave layer having the same index. The amplification coefficient must be different from zero ($C_2 \neq 0$) and bounded because if $C_2 = 0$, the systems of the slave layer will diverge and if C_2 is too large, the slaving factor will tend to zero. Therefore, we keep C_2 in the interval between 0.005 and 2. This type of topology finds applications in many domains such as aircraft control where recently they have proven that an optimal control permitted to regulate the air traffic in the sky.[31] Considering the domains of application of this network topology, it seems rather important to investigate the dynamics of this network with different parameters, which is presented in Sec. III.

III. DYNAMICS OF NETWORKS

A. Dynamics of different layers

Considering the topology given in Fig. 1 and the mathematical equations for both layers Eqs. (2) and (3), respectively, we are going to investigate numerically the dynamics in the different layers using the MSF described in Appendix B. A numerical calculation is done using Runge–Kutta fourth order method for a long time simulation, and the permanent solutions are considered at $t_{min} = 0.6\, t_{max}$.

To illustrate the behavior of the oscillators of the first layer, we present in Fig. 2(a) the master stability function or largest Lyapunov exponent (*LLE*) of the variational equation (B10) used to characterize the stability of the synchronization in the first layer. In this figure, there are two important regions in terms of characterization of the stability of the synchronization: if $LLE \leq 0$, the synchronization is stable and if $LLE > 0$, the synchronization is unstable. By varying smoothly the intralayer coupling ϵ_1, this figure shows that when ϵ_1 increases, the systems evolve to the synchronous state at $\epsilon_1 = 0.009$. This synchronization is obtained at a minimal value of the coupling strength in the first layer, and we note that the synchronization in the slave layer is highly influenced not only by the coupling but also by the amplification, this can be seen in the behavior of the order parameter,[32,33] which is plotted in Fig. 2(b) as a function of ϵ_1. The procedure to compute the order parameter is explained in Appendix C. It should be noted that the notion of amplification here is related to the amplitude of the oscillations of the state variables of the systems. We are talking about synchronization with amplification if and only if the ratio $X/Y = C_2$ is respected, as shown in Appendix A. So, we investigate here the impact of the amplification parameter on the dynamics of the network, where the order parameter of the slave layer is plotted for different values of C_2. According to this figure, although the interaction between the layers does not impede synchronization in the slave layer, it becomes more effective for small values of C_2. Based on the demonstration given in Appendix A, synchronization occurs at $Y = \frac{X}{C_2}$. Therefore, when $C_2 < 1$, we obtain an amplification in the slave layer and, respectively, a reduction in the master layer and vice versa when $C_2 > 1$. Thus, if we need to achieve synchronization in both layers at the same value of the interlayer coupling, C_2 must be very small, leading to a significant amplification at the second layer. Also from Fig. 2(b), we see that for the minimum value of $C_2 = 0.005$, the synchronization in both layers happens at the corresponding values of ϵ_1 and ϵ_2 ($\epsilon_2 = 10\epsilon_1$), this is represented in Fig. 2(b), where the order parameter r_1 and r_2 for both layers is seen to reach the value for complete synchronization at the same point. This value of C_2 produces amplification of around 200 of all the variables of the master layer ($Y \approx 200X$) in the slave layer. In Fig. 2(c), we plot the mean phase of the driver and the slave layer (the first 30 systems are for the driver layer and the rest for the slave layer) for the value $\epsilon_1 = 0.005$ of the intralayer coupling. The situation shown here is confirmed by Fig. 2(a) ($LLE > 0$). If we consider $\epsilon_1 = 0.007$, Fig. 2(a) shows that the largest Lyapunov exponent is non-negative but very close to zero, then in Fig. 2(d), we show the mean phase where the master layer has a two cluster synchronization with equal phases.[9,10,34–36] In the slave layer, while the clusters follow the systems with the same index as that of the master layer, we see an oblique sliding of the systems reminding of a splay state. To better appreciate the dynamics of the oscillators in this behavior, we show in Fig. 2(g), the attractors of the oscillators labeled $1, 6, 11, 16, 21, 26$ in the master and slave layers for $C_2 = 2$ and $\epsilon_1 = 0.007$ ($LLE \geq 0$). For $\epsilon_1 = 0.009$ (with $LLE < 0$), we obtain Fig. 2(e), which represents the synchronization in the first layer and a coherent oblique sliding in the second layer. By computing the phase difference between consecutive oscillators (here consecutive refers to the indices of the oscillators), we verified that the phase distance between oscillators of the consecutive index in the slave layer is constant; therefore, the second layer presents indeed a phenomenon of splay.[37,38] In Fig. 2(f), we show for $\epsilon_1 = 0.04$, the phase synchronization in both layers but not at the same value of the mean phase. So, for the multilayer network, the dynamics is equivalent to that of two clusters. To illustrate the dynamics of the system, we show in Fig. 2(h) the attractors of some oscillators (labeled $1, 6, 11, 16, 21, 26$) for $\epsilon_1 = 0.04$ to appreciate the behavior of the entire network.

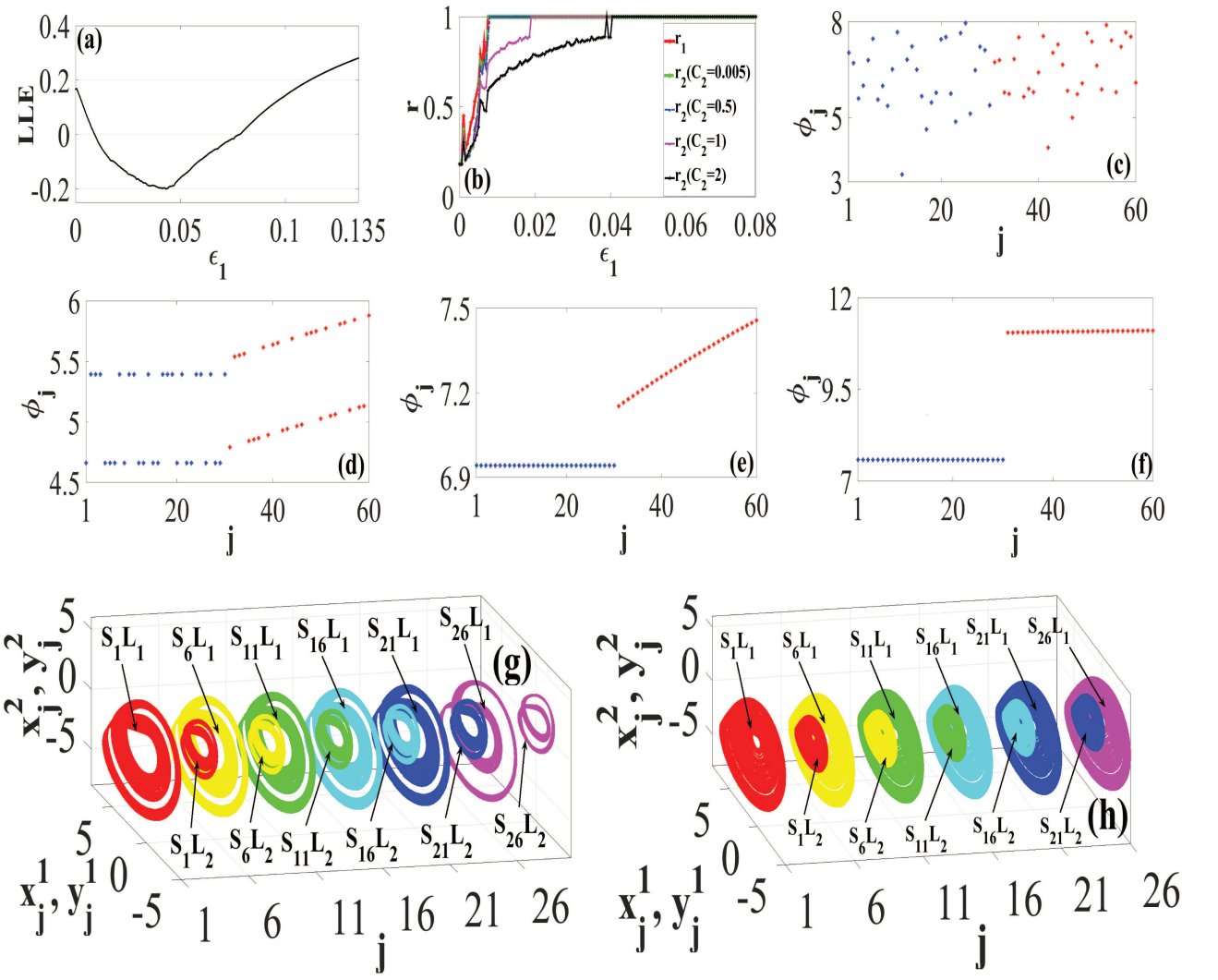

FIG. 2. Dynamics of the two layers of the network: (a) master stability function of the first layer as a function of the intralayer coupling considering $\epsilon_2 = 10\epsilon_1$, $C_0 = 1$, and $C_2 = 2$. (b) Order parameter showing the dynamics of the slave layer for different values of the amplification coefficient for $\epsilon_2 = 10\epsilon_1$ and $C_0 = 1$. (c)–(f) Mean phase of the first and second layer, respectively, for $\epsilon_1 = 0.005, 0.007, 0.009, 0.04$, $C_0 = 1$ and $C_2 = 2$. (g) Attractors of the oscillators 1, 6, 11, 16, 21, and 26 in the master and slave layer for $\epsilon_1 = 0.007$. (h) Attractors of the oscillators 1, 6, 11, 16, 21, and 26 in the master and slave layer $\epsilon_1 = 0.009$, respectively. S_iL_l means system i of layer l ($i = 1, 2, \ldots, N$ and $l = 1, 2$).

Therefore, we can conclude that according to the different values of the intralayer coupling, the network leads to different phenomena such as cluster synchronization, splay, synchronization, and the stability of this synchronization is confirmed by the MSF.

B. Impact of the interlayer coupling and amplification on the dynamics of the network

In Sec. III A, we have shown the influence of the intralayer coupling on the dynamics of the network. We see that the network presents many phenomena depending on the amplification coefficient C_2 and the interlayer coupling C_0. In this section, our goal is twofold: first, we investigate the behavior of the network under the impact of these two parameters and then we show the effect of the amplification as well as its effectiveness in the network. We keep the intra-coupling constants (ϵ_1, ϵ_2) fixed, varying smoothly the amplification coefficient (C_2) from 0.005 to 2 and the inter-coupling (C_0) from 0 to 20.

As mentioned in Fig. 2(b), the synchronization in the slave layer is imposed by the synchronization in the master layer. According to the literature,[39,40] in order to bring our multilayer network toward a desired behavior such as synchronization, cluster

formation, splay, and so on, it suffices to adjust the coupling. Although this is usually the case, in our system we have two important parameters acting as interlayer couplings (C_0 and C_2) with the difference that one of them (C_2) allows us to increase or decrease the amplitude of the signal in one of these layers. To illustrate the evolution toward the synchronization as a function of the amplification parameter C_2 and the interlayer coupling C_0 we show in Fig. 3(a) the order parameter of the slave layer, since we are interested in synchronization throughout the network. By considering the intralayer coupling $\epsilon_1 = 0.03$ and $\epsilon_2 = 0.25$ all the oscillators of the first layer are synchronized but due to the effects of the amplification parameter C_2 and the interlayer coupling, the dynamics of the slave layer cannot be the same. Therefore, the dynamics of the multilayer network and particularly the slave layer is greatly affected by C_0 and C_2. This can be observed in Fig. 3(a) where we plot the order parameter of the second layer. In red we represent the region where synchronization and amplification is obtained. We note that in this red zone the relation $X = C_2 Y$ is verified with a precision of 10^{-4}, while in the blue domain it is possible to obtain synchronization in the first layer only but not in both layers of the networks.

This information is corroborated by the number of states of the second layer shown in Fig. 3(b). This Fig. 3(b) confirms the order parameter by presenting a number of states equal to one in the case of synchronization (dark blue). When the order parameter is different from one, the synchronization of all the systems in the network is not achieved. At the moment, we can find partial synchronization called cluster which is characterized by a number of independent states of the network much less than the total number of elements. Based on Fig. 3(b), we see a thin region with cluster formation in the area of transition from synchronization to desynchronization and vice versa.

To better highlight the impact of the amplification (C_2) on the transition to synchronization, we have presented the order parameter of the multilayer network showing the transition to the synchronous state for three values of the amplification $C_2 = 0.5$, $C_2 = 1$ and $C_2 = 2$, showed in Figs. 3(c)–3(e), respectively. Varying smoothly the intra- and interlayer coupling for these three fixed values of C_2, we have obtained different areas of synchronization of the systems of the network. For these three figures, the first domain (D1) represents the region where there is no synchronization in any layer and the second domain (D2) where the synchronization exists only in the first layer. The third domain (D3) represents the zone of synchronization of both layers and the last domain (D4) is showing the area where there is the divergence between the states of the oscillators of the slave layer. Here, divergence means an infinite amplification of the amplitude of the oscillations of the systems of the slave layer leading to an explosion (y^1, y^2, y^3 tend toward the infinite). In summary, we notice that, the area of synchronization of both layers increases when the amplification coefficient decreases. So in Fig. 3(c) this zone of synchronization of both layers is the largest domain (D3) and the zone (D2) where only the master layer synchronizes is almost nonexistent. Therefore, when C_2 increases, it takes stronger values of the coupling in the master layer for the slave layer to become synchronized as can be seen in Fig. 2(b). Figure 4 is used to confirm and to present the transition to the synchronization using the Pearson correlation[41] [defined by Eq. (4)] between the first variables of each oscillator of both layers, the time series of the

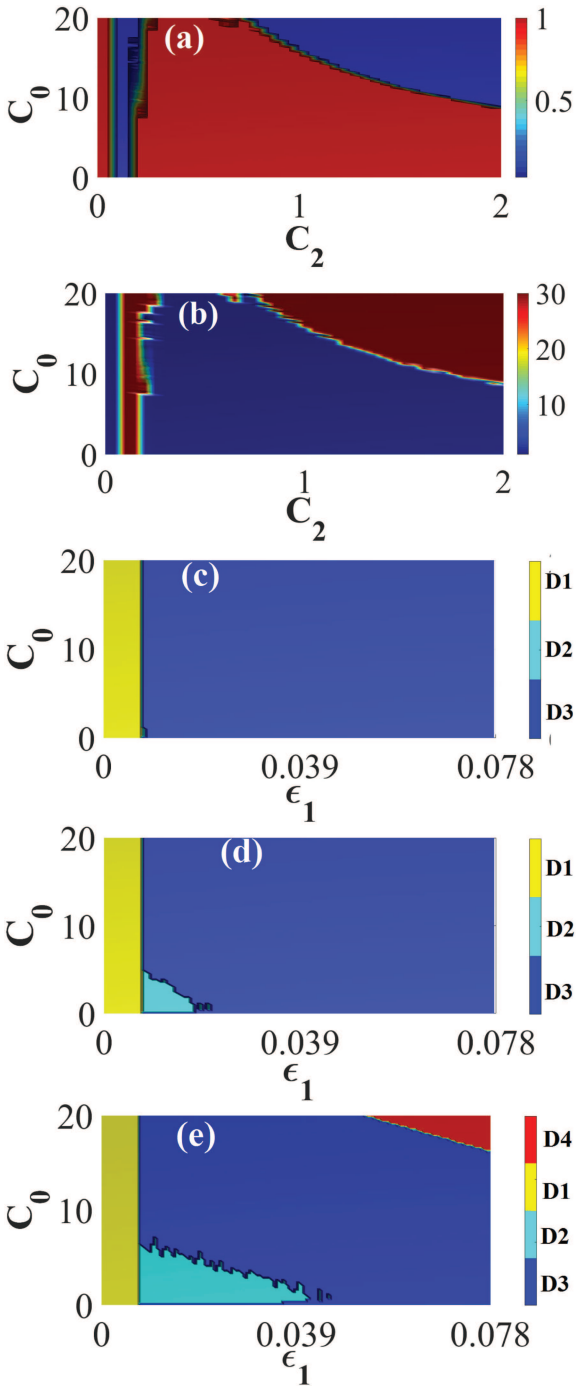

FIG. 3. Network synchronization regions: (a) order parameter of the multilayer network for $\epsilon_1 = 0.03$ and $\epsilon_2 = 0.25$ as a function C_0 and C_2. (b) Number of states in the slave layer for $\epsilon_1 = 0.03$ and $\epsilon_2 = 0.25$ as function C_0 and C_2. Two parameter phase diagram by simultaneously varying the intra-layer coupling ϵ_1 and inter-layer coupling C_0 with $\epsilon_2 = 10\epsilon_1$ and for different values of the amplification coefficient C_2: (c) $C_2 = 0.5$, (d) $C_2 = 1$, and (e) $C_2 = 2$.

first variables of the oscillator labels 1 and 15 of both layers, and the mean phase of the oscillators of the network,

$$\rho(x^1, y^1) = \frac{\sum_{i=1}^{N}(x_i^1 - \bar{x}^1)(y_i^1 - \bar{y}^1)}{\sqrt{\sum_{i=1}^{N}(x_i^1 - \bar{x}^1)^2}\sqrt{\sum_{i=1}^{N}(y_i^1 - \bar{y}^1)^2}}, \tag{4}$$

where $\bar{x}^1 = \sum_{i=1}^{N} x_i^1$ and $\bar{y}^1 = \sum_{i=1}^{N} y_i^1$ are the mean of the state variables x_i^1 and y_i^1. In this paper, the color yellow used in the correlation refers to the oscillators that synchronize and the color blue to those that do not synchronize.

Figure 4(a) shows the correlation between the first variables of the oscillators of the master and slave layer for $C_0 = 10$ and $C_2 = 0.2$ [these values are taken almost at the border of the separation of the red and blue zone in Fig. 3(a)]. This figure presents yellow and blue colors to identify those oscillators of the multilayer network that synchronize and those who do not synchronize, respectively. In this figure, the x-axis corresponds to the index used to identify the oscillators of the master layer (i) and the y-axis corresponds to the index used to identify the different oscillators of the slave layer (j). According to this figure, the first 14 oscillators of both layers synchronize. To present in detail the situation, we plot in Fig. 4(b) the same fixed values of the parameters and the mean phase for oscillators in both layers, where labels 1–30 belong to the master layer and 30–60 to the slave layer. Here, we notice two different groups in each layer: the synchronous group (first 14 oscillators of each layer) and the asynchronous group, so the transition to the synchronization is done by cluster formation. To show the effect of the amplification for these fixed values of parameters, we have in Fig. 4(c) the time series of the variables for oscillators labels 1 and 15. This figure presents a chaotic evolution of these variables as a function of time as well as amplification, these effects of synchronization with amplification are well appreciated in Figs. 4(d) and 4(f) for the oscillators indicated in the axes. According to Fig. 4(a), the 15th oscillator of the master layer and the 14th oscillator of the slave layer cannot synchronize [see Fig. 4(e)]. At the end, to confirm the synchronization with amplification in the multilayer network, we present in Fig. 4(g) the correlation between the elements of both layers for $C_0 = 10$ and $C_2 = 1.55$. This correlation shows the synchronization of the multilayer network, which can be appreciated in Fig. 4(h) where we plot the mean phase for oscillators in both layers. The time series of the oscillators 1 and 15 [Fig. 4(i)] show the amplification described in Eq. (3). We can appreciate the synchronization with the amplification of the multilayer network in the Figs. 4(j)–4(l), where complete synchronization of some chosen oscillators is shown.

To appreciate the dynamics at the border of the separation of the domain D3 and D4 of Fig. 3(e), we present in Fig. 5(a), the variation of the phase of all oscillators of the slave layer for $C_2 = 2$, $\epsilon_1 = 0.065\,721$, $\epsilon_2 = 10\epsilon_1$, and interlayer coupling (C_0) varying from 17.8 to 18.2. At this range of values of the interlayer coupling, the slave layer presents different dynamics. Before $C_0 = 18$, this slave layer shows the synchronization of all oscillators of the slave layer. After this synchronization, there follows a slight zone of disturbance [the zoom is given in Fig. 5(b)] before the division into two groups, which drives the layer toward the divergence. This abrupt change presented reminds of an explosive desynchronization.[11] Given the form of the connection (unidirectionnal coupling) between the first and second layers, the oscillators of the slave layer can only remain synchronous and stable for a certain range of values of C_0. This dynamic leads the slave layer to the divergence that we observe in Fig. 5(a) on the mean phase and in Fig. 5(c) with the order parameter. To understand more clearly the dynamics of the slave layer at this value of interlayer coupling where we have the destruction of the synchronization, we show in Figs. 5(d) and 5(e) the mean phase of the multilayer network and the correlation between the oscillators of the slave layer, respectively. The mean phase presents a phase synchronization of all the oscillators of the first layer, but in the slave layer, we have two clusters formations. This cluster formation in the slave layer is confirmed using the correlation between the oscillators of the slave layer, and then we can appreciate the formation of these two clusters by the yellow color.

IV. APPLICATIONS TO OTHER SYSTEMS

The behavior of a multilayer network shown in Secs. II and III is not restricted to a system of Rössler oscillators, it can also be obtained with other systems and topologies. In this section, we shall study a network of jerk oscillators and another of Liénard oscillators with different topologies and show that they reproduce the same behaviors.

A. Synchronization with amplification in a multilayer network of jerk oscillators

Here, we investigate the dynamics of a multilayer network of jerk[50] chaotic oscillators where the first layer is described by Eq. (5),

$$\begin{cases} \dot{x}_i^1 = I(x_i^2) + \epsilon_1(x_{i+1}^1 + x_{i-1}^1 - 2x_i^1), \\ \dot{x}_i^3 = \alpha(-x_i^3 + I(x_i^2)), \\ \dot{x}_i^3 = \beta(-x_i^2 + x_i^2 - \gamma x_i^3). \end{cases} \tag{5}$$

The slave layer is described by Eq. (6)

$$\begin{cases} \dot{y}_j^1 = \dfrac{I(x_j^2)}{C_2} + \epsilon_2(y_{j+1}^1 + y_{j-1}^1 - 2y_j^1) + C_0(x_j^1 - C_2 y_j^1), \\ \dot{y}_j^2 = \alpha(-y_j^3 + I(x_j^2)/C_2), \\ \dot{y}_j^3 = \beta(-y_j^1 + y_j^2 - \gamma y_j^3). \end{cases} \tag{6}$$

Where the piecewise linear function is

$$I(x^2) = \begin{cases} -x^2 & \text{if } x^2 \le 1, \\ -1 & \text{otherwise.} \end{cases} \tag{7}$$

$\alpha = 0.025$, $\beta = 0.765$, $\gamma = 0.0938$ are the systems parameter. ϵ_1 and ϵ_2 are the intralayer coupling strength of the drive and slave layer of the network. The connection between the nodes of the same layer is bidirectional, and they are arranged on a ring. Moreover, the connection between the nodes of different layers is unidirectional and it only concerns the oscillators with the same index in both layers.

Equations (5) and (6) were solved numerically considering $N = 30$ jerk oscillators per layer with the systems parameter defined above. Figure 6 is obtained for $\epsilon_1 = 2$, $\epsilon_2 = 2$, and $C_0 = 2$. Two values for the amplification coefficient are considered: $C_2 = 0.5$ and $C_2 = 2$. For $C_2 = 0.5$, we can clearly appreciate in Fig. 6(a) the complete phase synchronization of all oscillators in both layers. This

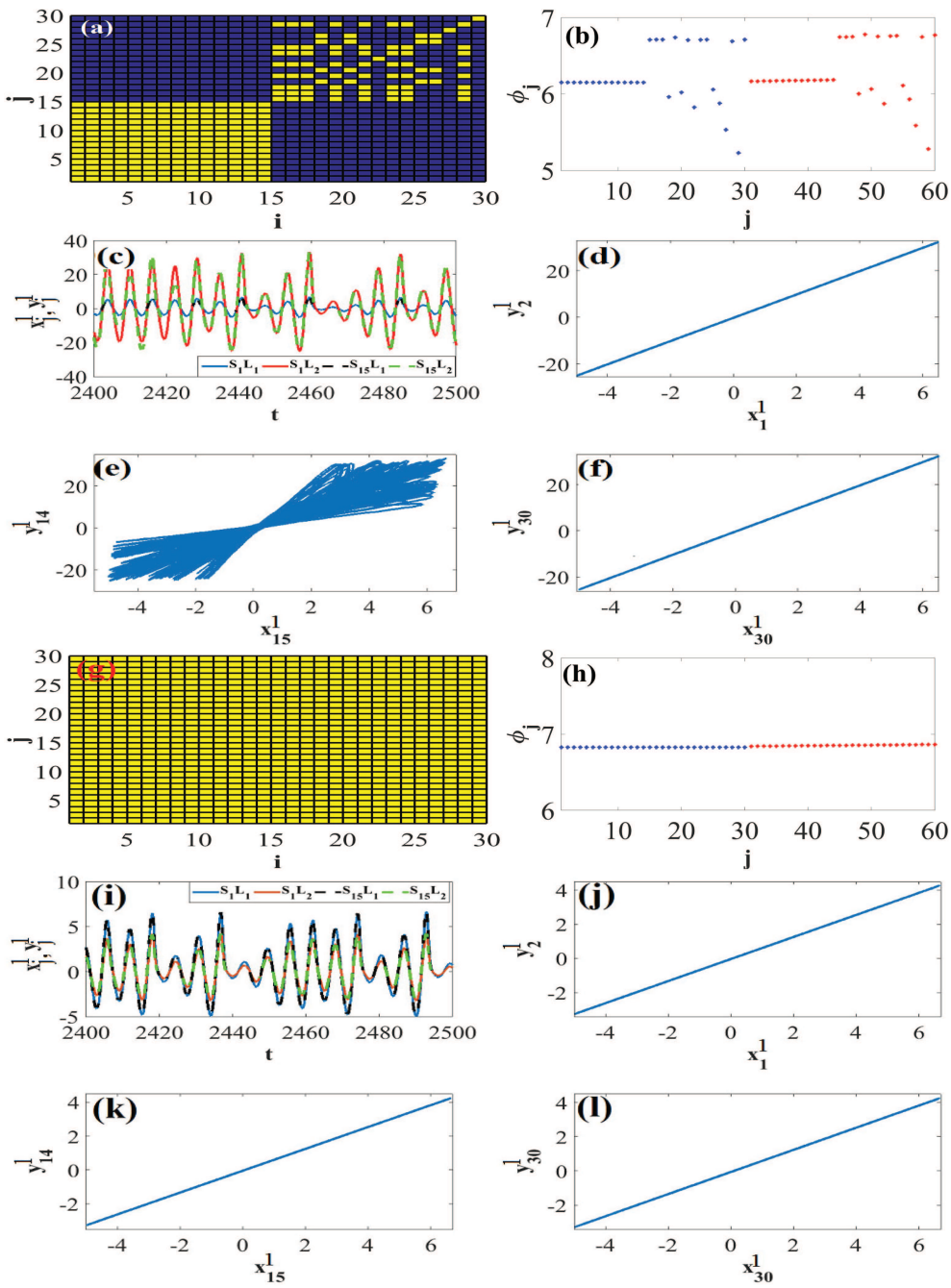

FIG. 4. Dynamics of the multi-layer network for C_0 and C_2: (a) correlation between x_i^1 and y_j^1 (the yellow color indicates the oscillators in the synchronized state, and the blue oscillators in an unsynchronized state). (b) Mean phase and (c) time series of some oscillators of the network for $C_2 = 0.2$ and $C_0 = 10$. S_iL_l means system i of the layer l (i = 1, 2,…, N and l = 1, 2). (d)–(f) Synchronization between some oscillators in the first and second layers of the network for $C_2 = 0.2$ and $C_0 = 10$. (g) Correlation between x_i^1 and y_j^1. (h) Mean phase and (i) time series of some oscillators of the network for $C_2 = 1.55$ and $C_0 = 10$. (j)–(l) Synchronization between some oscillators in the first and second layers of the network for $C_2 = 1.55$ and $C_0 = 10$. Figures (d)–(f) and (j)–(l) are special cases of the correlations presented in Figs. 4(b) and 4(g). However, these figures even if they may confuse for being similar show that amplification clearly depends on the value of C_2 and also show that in some cases, the synchronization of oscillators of different indices is possible [see Figs. 4(d) and 4(k)].

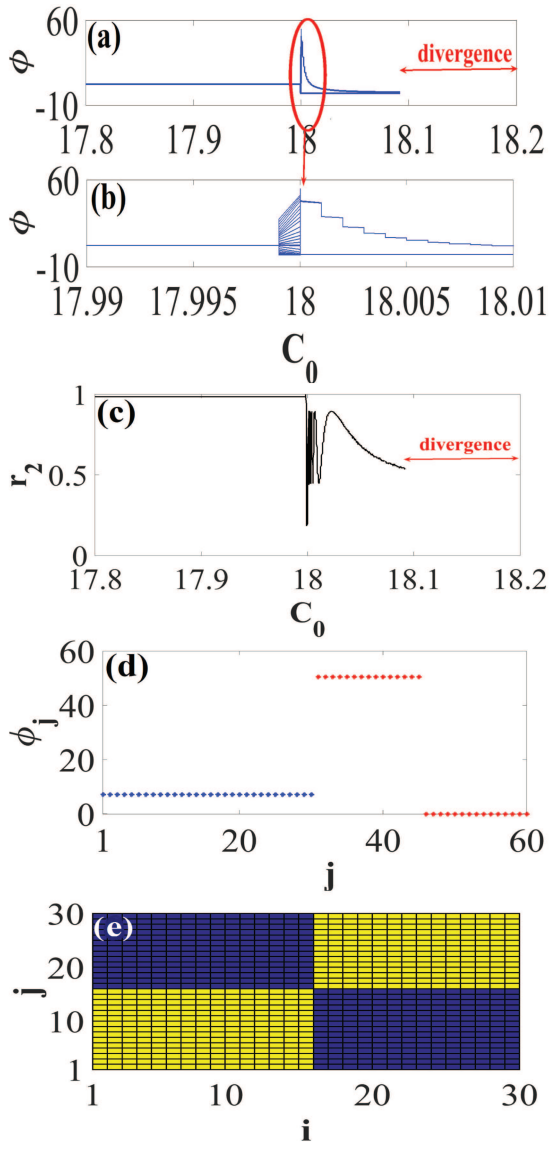

FIG. 5. Road to divergence: (a) Variation of the phases of the slave layer for $C_2 = 2$, $\epsilon_1 = 0.065\,721$ and $\epsilon_2 = 10\epsilon_1$. (b) Zoom of the variation of the phases of the slave layer for $C_2 = 2$, $\epsilon_1 = 0.065\,721$ and $\epsilon_2 = 10\epsilon_1$. (c) Order parameter of the slave layer for $C_2 = 2$, $\epsilon_1 = 0.065\,721$ and $\epsilon_2 = 10\epsilon_1$. (d) Mean phase of the oscillators of the network and (e) correlation between the oscillators of the slave layer for $\epsilon_1 = 0.065\,721$ and $\epsilon_2 = 10\epsilon_1$, $C_2 = 2$ and $C_0 = 18$. (The yellow color indicates the oscillators that synchronize, and the blue color those that do not synchronize.)

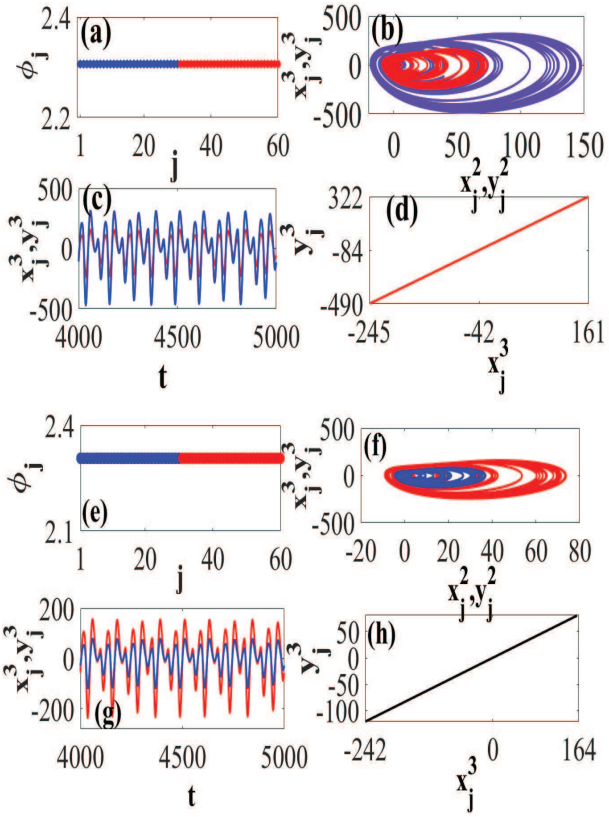

FIG. 6. Dynamics of the two layers of the network of jerk oscillators, where the master layer is represented in red and the slave layer in blue. For $\epsilon_1 = \epsilon_2 = 2$, $C_0 = 5$ and $C_2 = 0.5$: (a) mean phase of the first and second layers, (b) attractors of the oscillators in the master and slave layer, (c) time series of the oscillators of the master and slave layer, and (d) synchronization between the oscillators of the first and second layers in the network. For $\epsilon_1 = \epsilon_2 = 2$, $C_0 = 5$ and $C_2 = 2$: (e) mean phase of the first and second layers, (f) attractors of the oscillators in the master and slave layer, (g) time series of the oscillators of the first and second layers, and (h) synchronization between the oscillators of the first and second layers in the network.

phase synchronization is a major condition to obtain amplification in the systems of the network. As defined by our model, it emerges that for these values of C_2, the oscillators of the slave network are supposed to be amplified compared to oscillators of the master layer [see Figs. 6(b) and 6(c), where in red, we show the oscillators of the master layer and in blue those of the slave layer]. The amplification between the master and slave layers is perfectly observed in Fig. 6(d). In the second case, we consider $C_2 = 2$. As in the previous case, we have phase synchronization between the oscillators of both layers [see Fig. 6(e)]. For this value, we have amplification in the oscillators of the master layer [see Figs. 6(f) and 6(g)]. In the same vein, we present in Fig. 6(h) the synchronization between the oscillators in the first and second layers of the network.

Therefore, interlayer synchronization can be obtained with amplification or reduction depending on the value of coefficient C_2.

B. Chimera states with amplification in a multilayer network of the Liénard system

Let us consider a network of Liénard systems expressed as in Ref. 15, where the authors chose to investigate the dynamics of the

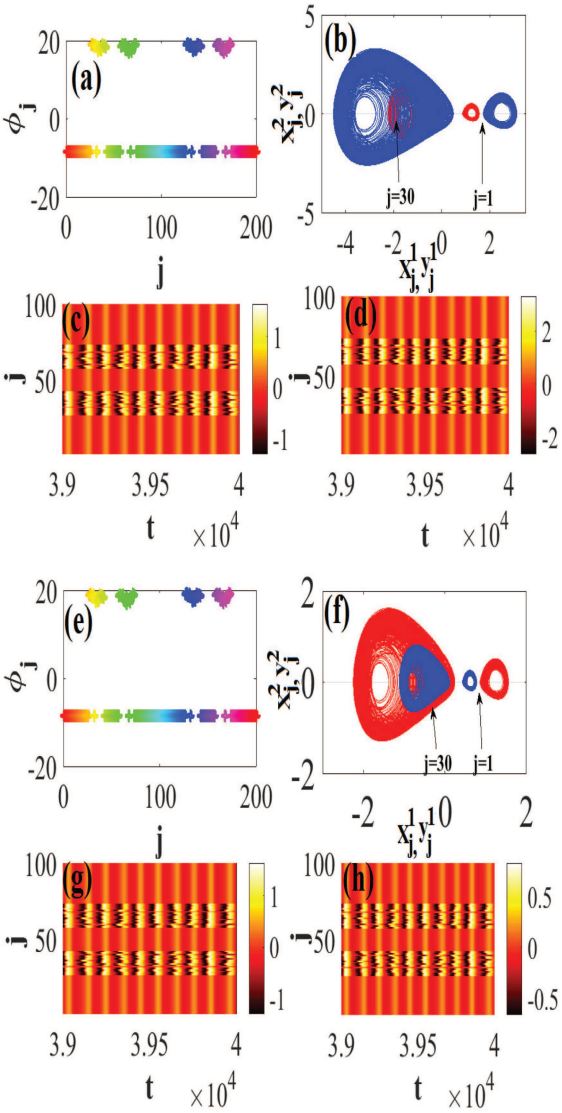

FIG. 7. Examples of behavior of the multilayer network of Liénard systems. Amplification for $K = 0.9$, $\epsilon_1 = \epsilon_2 = -0.57$, $C_2 = 0.5$: (a) Snapshot of all the oscillators of the multilayer network showing a multichimera state, (b) phase portrait of the oscillators $j = 1$ and $j = 30$ of both layers, and (c) and (d) temporal dynamics of all the nodes in the first and second layers in the network. Reduction for $K = 0.9$, $\epsilon_1 = \epsilon_2 = -0.57$, $C_2 = 2$, (e) snapshot of all the oscillators of the multilayer network showing a multichimera state, (f) phase portrait of the oscillators $j = 1$ and $j = 30$ of both layers and (g) and (h) temporal dynamics of all the nodes in the first and second layers in the network.

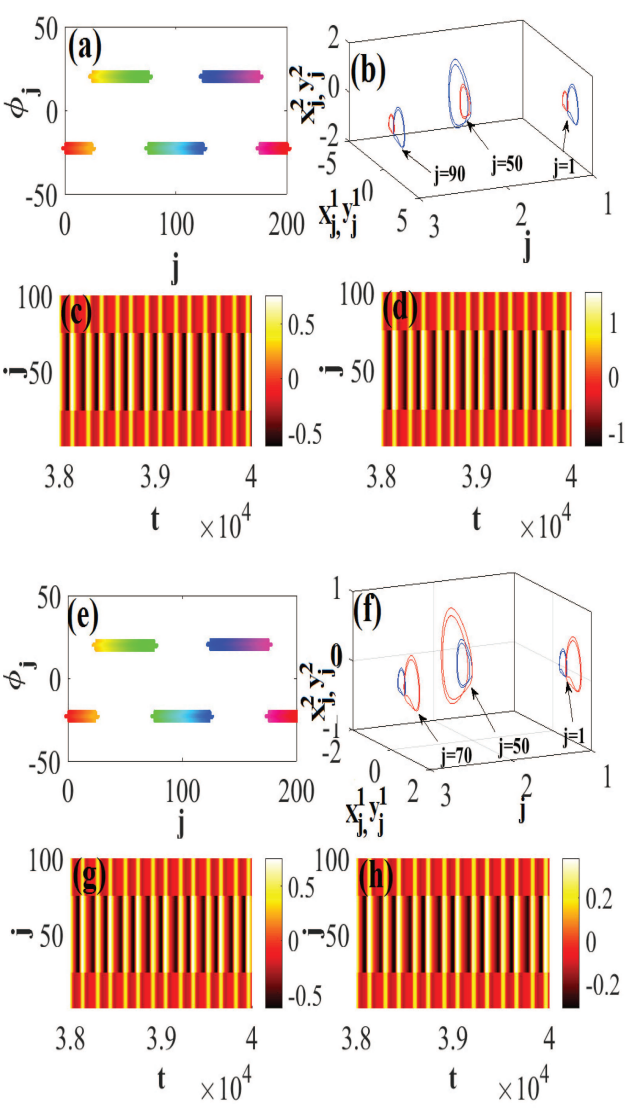

FIG. 8. Examples of the behavior of the multilayer network of Liénard systems. Amplification for $K = 1.5$, $\epsilon_1 = \epsilon_2 = -0.1$, $C_2 = 0.5$: (a) Snapshot of all the oscillators of the multilayer network showing a cluster, (b) phase portrait of the oscillators $j = 1$, $j = 50$, and $j = 90$ of both layers, and (c) and (d) temporal dynamics of all the nodes in the first and second layers in the network. Reduction for $K = 1.5$, $\epsilon_1 = \epsilon_2 = -0.17$, $C_2 = 2$. (e) Snapshot of all the oscillators of the multilayer network showing a cluster, (f) phase portrait of the oscillators $j = 1$, $j = 50$, and $j = 70$ of both layers, and (g) and (h) temporal dynamics of all the nodes in the first and second layers in the network.

oscillators basing themselves on an attractive and repulsive global coupling. In the same vein, in Refs. 42 and 43, the authors present some behavior such as clusters, pattern formation, synchronization, and so on according to the attractive and repulsive coupling.

In this subsection, we consider the Liénard model with a intralayer topology defined as in Ref. 15.

First or master layer,

$$\begin{cases} \dot{x}_i^1 = x_i^2, \\ \dot{x}_i^2 = -\alpha x_i^1 x_i^2 - \beta (x_i^1)^3 - \gamma x_i^1 + K\left[\left(\bar{x}^2 - x_i^2\right) + \epsilon_1 \left(\bar{x}^1 - x_i^1\right)\right], \end{cases} \tag{8}$$

where $\bar{x}^1 = \frac{1}{N}\sum_{i=1}^{N} x_i^1$ and $\bar{x}^2 = \frac{1}{N}\sum_{i=1}^{N} x_i^2$.

Second or slave layer,

$$\begin{cases} \dot{y}_j^1 = y_j^2 + C_0(x_i^1 - C_2 y_j^1), \\ \dot{y}_j^2 = -\alpha \dfrac{x_j^1 x_j^2}{C_2} - \beta \dfrac{(x_i^1)^3}{C_2} - \gamma y_j^1 + K\left[\left(\bar{y}^2 - y_j^2\right) + \epsilon_2\left(\bar{y}^1 - y_j^1\right)\right] + C_0(x_j^2 - C_2 y_j^2), \end{cases} \tag{9}$$

with $\bar{y}^1 = \frac{1}{N}\sum_{i=1}^{N} y_i^1$ and $\bar{y}^2 = \frac{1}{N}\sum_{i=1}^{N} y_i^2$.

The system's parameters α, β, and γ are selected exactly as in Ref. 15, K is the strength of coupling, ϵ_1 and ϵ_2 are the intralayer global mean field coupling, and C_2 is the amplification coefficient. The coupling between the nodes of different layers is unidirectional and it only concerns the oscillators with the same index in both layers and $N = 100$ Liénard systems.

For the numerical simulation, we consider two cases, one where the amplification is less than 1 (the systems of the slave layer are amplified and the systems of the master layer are reduced) and another when the amplification is greater than 1 (the systems of the slave layer are reduced and the systems of the master layer are amplified).

Figure 7 elaborates the chimera-I states based on Refs. 15 and 16. Figure 7(a) presents a snapshot of all the oscillators of both layers of the network (the first 100 systems correspond to the master layer and the rest is for the slave layer). This figure presents a multichimera state in both master and slave layers [see Figs. 7(c) and 7(d)] and a phase synchronization of both layers for $K = 0.9$, $\epsilon_1 = \epsilon_2 = -0.57$, and $C_2 = 0.5$. For the same parameters, we show in Fig. 7(b), the attractor of the system for oscillator $j = 1$ in the synchronization state and the attractor for $j = 30$ in the incoherent state for both layers of the network (attractor red corresponds to the master layer and attractor blue for the slave layer). At $C_2 = 0.5$, the systems of the slave layer are supposed to be amplified as in Fig. 7(b). In the same vein, we present in Figs. 7(e)–7(h) for $C_2 = 2$, the same behaviors as in Figs. 7(a)–7(d). We observe the same behaviors except that are the systems of the master layer, which are amplified as $X = 2Y$.

Based on these results, we conclude that this form of coupling can lead to a chimera or multichimera state with amplification or reduction depending on the value of the amplification coefficient.

Let us now consider the following parameters $K = 1.5$ $\epsilon_1 = \epsilon_2 = -0.1$ that lead to a cluster formation and we choose two values of amplification parameter: (a) $C_2 = 0.5$ [see Figs. 8(a)–8(d)] and (b) $C_2 = 2$ [see Figs. 7(e)–7(h)]. According to these two cases, we notice that this cluster state can be maintained with amplification or reduction based on the value of C_2.

V. CONCLUSION

Summarizing, we have studied and characterized numerically the synchronization and the amplification of signals in a multilayer network of Rössler, jerk, or Liénard oscillators. Using tools for studying synchronization in the network such as a master stability function, the order parameter, we have demonstrated that the existence of synchronization in the second layer is conditioned by the first. To obtain synchronization of both layers at the same value of the intralayer coupling, the amplification coefficient must be sufficiently low [see Fig. 2(b)]. The key role of amplification is demonstrated by analyzing the order parameter of the first and second layers. This parameter leads the network to different dynamics such as cluster formation and synchronization.

From a theoretical point of view, this work contributes to the advancement in the understanding of the phenomenon of synchronization and amplification of signals between two coupled networks. From a practical point of view, the results may be useful in many technological applications. For example, in several mechanical systems, the transmission of movements or orders is done through a driving belt or gear.[44] Concerning this process, one of the most important parameters is the transmission ratio, here represented by C_2, the amplification parameter. The amplification coefficient could be the transmission ratio between gears or pulley-belt systems.[45]

ACKNOWLEDGMENTS

H.A.C. acknowledges ICTP-SAIFR and FAPESP Grant No. 2016/01343-7 for partial support. V.C. and F.F.F. acknowledge finance support, in part, by the Coordenação de Aperfeiçoamento de Pessoal de Nível Superior—Brasil (CAPES)—Finance Code No. 001.

APPENDIX A: SYNCHRONIZATION CONDITIONS

We consider $X(x_i^1, x_i^2, x_i^3)$ and $Y(y_i^1, y_i^2, y_i^3)$, the state vector of the ith oscillator of the first and second layer, respectively.

The dynamics of the first and second layers are given, respectively, by

$$\begin{cases} \dot{x}_i^1 = -x_i^2 - x_i^3 + \epsilon_1 \sum_{k=1}^{N} A_{ik}^1 (x_k^1 - x_i^1), \\ \dot{x}_i^2 = x_i^1 + a x_i^2, \\ \dot{x}_i^3 = b x_i^1 + x_i^3 (x_i^1 - c) \end{cases} \tag{A1}$$

and

$$\begin{cases} \dot{y}_j^1 = -y_j^2 - y_j^3 + \epsilon_2 \sum_{k=1}^{N} A_{jk}^2 (y_k^1 - y_j^1) + C_0(x_j^1 - C_2 y_j^1), \\ \dot{y}_j^2 = \dfrac{x_j^1 + a x_j^2}{C_2}, \\ \dot{y}_j^3 = b y_j^1 + \dfrac{x_j^3 x_j^1}{C_2} - c y_j^3. \end{cases} \tag{A2}$$

Without any intralayer coupling ($\epsilon_1 = \epsilon_2 = 0$), both layers could synchronize with amplification depending on C_2.

We consider the synchronization error $e = X - C_2 Y$ with $\epsilon_1 = \epsilon_2 = 0$. So, the error dynamical system, which is obtained only for a couple of systems with the same index in the first and second

layers, is given by Eq. (A3)

$$\begin{cases} \dot{e}_i^1 = -e_i^2 - e_i^3 - C_2 C_0 e_i^1, \\ \dot{e}_i^2 = 0, \\ \dot{e}_i^3 = b e_i^1 - c e_i^3. \end{cases} \tag{A3}$$

To simplify the demonstration, we consider the Lyapunov functions $v_i (i = 1, 2, \ldots, N)$ of system pairs i and j (with $i = j$) of the first and second layer described as follows:

$$v_i = \frac{1}{2}\left((e_i^1)^2 + (e_i^2)^2 + \frac{1}{b}(e_i^3)^2 \right). \tag{A4}$$

For any couple (X, Y), we choose the following Lyapunov function candidate:

$$v = \frac{1}{2}\left((e^1)^2 + (e^2)^2 + \frac{1}{b}(e^3)^2 \right). \tag{A5}$$

It is established (assuming $a > 0, b > 0$, and $c > 0$) that the system defined by Eq. (A3) is practically stable since the time derivative of the Lyapunov function in Eq. (A5) is bounded by a positive constant. This also means that the error between the driver and response systems is sufficiently small but different from zero and could be considered as tolerance in the synchronization condition,[46]

$$\dot{v} \leq \frac{(e^2)^2}{4c}. \tag{A6}$$

For the whole network, the Lyapunov function candidate V can be defined as a sum of v_i,

$$V = \sum_{i=1}^{N} v_i. \tag{A7}$$

Then, for the whole network, we can have

$$\dot{V} \leq \sum_{i=1}^{N} \frac{(e_i^2)^2}{4c}. \tag{A8}$$

Based on Eq. (A3), this boundedness is ensured by the fact that $e_i^2(t)$ is constant due to the fact that $\dot{e}_i^2(t) = 0$. Thereby, from Eq. (A8) $e \to 0$, $X - C_2 Y = 0$ and induce $X = C_2 Y$. we can obtain amplification or reduction depending on the value of the coefficient C_2.

APPENDIX B: PRELIMINARIES TO THE INVESTIGATION OF THE DYNAMICS OF THE NETWORK: THE MASTER STABILITY FUNCTION

A regular problem that arises when analyzing the dynamics of a network is to find conditions that guarantee the synchronization of a system of coupled identical nonlinear oscillators so that all the oscillators converge asymptotically toward the same state.

The Master Stability Function (MSF) developed by Pecora and Carroll[20] constitutes one of the most useful tools to analyze the synchronization stability of a system of coupled identical nonlinear oscillators.[1,20,47] We develop here only some points of the principal idea of this method.

Considering a network of N identical coupled chaotic oscillators (or nodes), let $\mathbf{x}_i$ be a vector with m components necessary to describe the state of the ith node. In general, in the absence of any interaction between the nodes of the network, the evolution of a node is given by Eq. (B1),

$$\dot{\mathbf{x}}_i = \mathbf{F}(\mathbf{x}_i). \tag{B1}$$

In this Eq. (B1), $\mathbf{F}$ is a function defined from $\mathbb{R}^m$ to $\mathbb{R}^m$ and is used to define the local dynamics of the oscillators. To describe how the oscillators evolve when they are connected in a network, we need to consider not only the local dynamics presented at Eq. (B1), but also how each node is affected by the ones to which it is connected. So, the law governing the dynamical interaction of the ith node is defined as

$$\dot{\mathbf{x}}_i = \mathbf{F}(\mathbf{x}_i) + \sigma \sum_{j=1}^{N} \mathbf{G}_{ij} \mathbf{H}(\mathbf{x}_j), \tag{B2}$$

where σ is a coupling strength, $H : \mathbb{R}^m \longrightarrow \mathbb{R}^m$ is an arbitrary output function of each node's variables used in the coupling. If we put the network in a synchronized state, we have $\mathbf{x}_i = \mathbf{s}$ for all nodes, where $\mathbf{s}$ is any m-dimensional vector. The only way all nodes have the same behavior is to have the sum, $\sum_{j=1}^{N} \mathbf{G}_{ij}$, be the same for all i. So, to obtain complete or identical synchronization, the row sums of the coupling matrix must be the same for all rows. According to Pecora and Carrol,[20] we can collect the node dynamical variables, functions, and coupling in

$$\mathbf{x} = [\mathbf{x}_1, \mathbf{x}_2, \ldots, \mathbf{x}_N], \tag{B3a}$$

$$\mathbf{F}(\mathbf{x}) = [\mathbf{F}(\mathbf{x}_1), \mathbf{F}(\mathbf{x}_2), \ldots, \mathbf{F}(\mathbf{x}_N)], \tag{B3b}$$

$$\mathbf{H}(\mathbf{x}) = [\mathbf{H}(\mathbf{x}_1), \mathbf{H}(\mathbf{x}_2), \ldots, \mathbf{H}(\mathbf{x}_N)], \tag{B3c}$$

and G be the matrix coupling coefficients G_{ij}, then based on Eqs. (B3a)–(B3c), Eq. (B2) can be written in a compact form as follows:

$$\dot{\mathbf{x}} = \mathbf{F}(\mathbf{x}) + \sigma \mathbf{G} \otimes \mathbf{H}(\mathbf{x}), \tag{B4}$$

where $\otimes$ is the Kronecker product. So, according to the form of Eq. (B2), we can rewrite Eq. (2) in the same form,

$$\mathbf{F}(\mathbf{x}_i) \begin{cases} \dot{x}_i^1 = -x_i^2 - x_i^3, \\ \dot{x}_i^2 = x_i^1 + a x_i^2, \\ \dot{x}_i^3 = b x_i^1 + x_i^3 (x_i^1 - c). \end{cases} \tag{B5}$$

According to Ref. 20, for an all-to-all coupling scheme, the connectivity matrix can be defined as in matrix G. To couple the nodes of the layer, we choose $\mathbf{x}^1$ component and then matrix H can be defined as in Eq. (B6),

$$\mathbf{H} = \begin{pmatrix} 1 & 0 & 0 \\ 0 & 0 & 0 \\ 0 & 0 & 0 \end{pmatrix},$$

$$\mathbf{G} = \begin{pmatrix} 1-N & 1 & \cdots & 1 & 1 & 1 \\ 1 & 1-N & \cdots & 1 & 1 & 1 \\ \vdots & \vdots & \cdots & \vdots & \vdots & \vdots \\ 1 & 1 & \cdots & 1 & 1-N & 1 \\ 1 & 1 & \cdots & 1 & 1 & 1-N \end{pmatrix}. \tag{B6}$$

The master stability function studies the stability of the global synchronization in the network. Therefore, the synchronous state is obtained when $\mathbf{x}_1 = \mathbf{x}_2 = \cdots = \mathbf{x}_N = \mathbf{s}$.

Suppose our system is synchronized and we perturb it so that each node is, in general, slightly "away" from the synchronized motion. Let us consider ξ_i a small perturbation of the ith node of the network so that after perturbation $\mathbf{x}_i = \mathbf{s} + \xi_i$. For N oscillators of the first layer, the collections of the variations can be expressed as $\xi = (\xi_1, \xi_2, \ldots, \xi_N)$. Now, we can derive an equation of motion for the small perturbations that we will use to explore if the synchronized state is unstable or stable. So, replacing the perturbation $\mathbf{x}_i = \mathbf{s} + \xi_i$ in Eq. (B2) and using the Taylor theorem expand of $\mathbf{F}(\mathbf{s} + \xi_i)$ and $\mathbf{H}(\mathbf{s} + \xi_i)$ to first order (since ξ_i is small), we have the following variational equation:

$$\dot{\boldsymbol{\xi}}_i = \mathbf{DF}(\mathbf{s})\xi_i + \sigma \sum_{j=1}^{N} \mathbf{G}_{ij}\mathbf{DH}(\mathbf{s})\xi_j. \tag{B7}$$

Using the tensor notation, we can write Eq. (B7) in a more compact form,

$$\dot{\boldsymbol{\xi}} = \left[\mathbf{1_N} \otimes \mathbf{DF}(\mathbf{s}) + \sigma \mathbf{G} \otimes \mathbf{DH}(\mathbf{s})\right]\xi, \tag{B8}$$

where $\mathbf{1_N}$ is the identity matrix of order N and $\mathbf{DF}$ and $\mathbf{DH}$ are the $N \times N$ Jacobian matrices of the corresponding vector functions.

The solution of Eq. (B8) can be in the form $\xi_i \sim \exp \mu_i t$. The exponents μ tell us if the perturbation grows ($\mu > 0$) or shrinks ($\mu < 0$), the former indicating a direction that is unstable and the latter a stable direction. After diagonalization of the second term of Eq. (B8), we obtain the variational equations which are diagonal in the node coordinates and are now uncoupled and individually given by

$$\dot{\boldsymbol{\xi}}_\mathbf{k} = \left[\mathbf{DF}(\mathbf{s}) + \sigma\alpha_k D\mathbf{H}(\mathbf{s})\right]\xi_k, \tag{B9}$$

where α_k is an eigenvalue of $\mathbf{G}$, $k = 1, 2, \ldots, N$. For each k, the form of each block of Eq. (B8) does not change, only the scalar multiplier $\sigma\alpha_k$ differs for each block.

Therefore, these steps lead us to design the following master stability equation:

$$\dot{\boldsymbol{\xi}} = \left[\mathbf{DF}(\mathbf{s}) + \sigma\alpha\mathbf{DH}(\mathbf{s})\right]\xi. \tag{B10}$$

Computing the largest Lyapunov exponent of this master stability equation Eq. (B10), we obtain what Pecora and Carroll called the master stability function and, therefore, we achieve a stable synchronization state if the MSF turns negative.[20,48,49]

APPENDIX C: CALCULATION OF THE ORDER PARAMETER

Collective behavior of such an N-oscillator system is conveniently described by the order parameter. The evaluation of this order parameter[12] used the phase of each oscillator of the network. To define the phase let us consider an arbitrary signal $s(\tau)$ with time τ and its Hilbert transformation to be $\tilde{s}(\tau)$, we have

$$\psi(\tau) = s(\tau) + i\tilde{s}(\tau) = R(\tau)\exp^{i\phi(\tau)}, \tag{C1}$$

where $R(\tau)$ is the amplitude and $\phi(\tau)$ the phase of the variable $s(\tau)$. If the instantaneous phase is $\phi_i(\tau)$, it can be determined through the following relation:

$$\phi_i(\tau) = \tan^{-1}\left[\frac{\tilde{s}_i(\tau)}{s_i(\tau)}\right]. \tag{C2}$$

In this paper, the calculation of the phase was carried out using, in each case, the variable that best describes the dynamics of the system.

Thus, from the expression of the phase ϕ_i, the mean phase ϕ is an algebraic average calculated on the N oscillators of the layer. So, for a network of N oscillators, the order parameter can be expressed as

$$r = \frac{1}{N}\sum_{i=1}^{N} e^{j\phi_i}, \tag{C3}$$

where $j^2 = -1$, when $r \to 1$, phase synchronization is reached and when $r \approx 0$, the network is desynchronized.

DATA AVAILABILITY

The data that support the findings of this study are available within this article.

REFERENCES

[1] I. Leyva, I. Sendiña-Nadal, R. Sevilla-Escoboza, V. Vera-Avila, P. Chholak, and S. Boccaletti, "Relay synchronization in multiplex networks," Sci. Rep. **8**, 1 (2018).
[2] M. De Domenico, A. Solé-Ribalta, E. Cozzo, M. Kivelä, Y. Moreno, M. A. Porter, S. Gómez, and A. Arenas, "Mathematical formulation of multilayer networks," Phys. Rev. X **3**, 041022 (2013).
[3] X. Zhang, S. Boccaletti, S. Guan, and Z. Liu, "Explosive synchronization in adaptive and multilayer networks," Phys. Rev. Lett. **114**, 038701 (2015).
[4] S. Jalan, A. D. Kachhvah, and H. Jeong, "Explosive synchronization in multilayer dynamically dissimilar networks," J. Comput. Sci. **46**, 101177 (2020).
[5] I. Belykh, D. Carter, and R. Jeter, "Synchronization in multilayer networks: When good links go bad," SIAM J. Appl. Dyn. Syst. **18**, 2267 (2019).
[6] K. A. Blaha, K. Huang, F. Della Rossa, L. Pecora, M. Hossein-Zadeh, and F. Sorrentino, "Cluster synchronization in multilayer networks: A fully analog experiment with L C oscillators with physically dissimilar coupling," Phys. Rev. Lett. **122**, 014101 (2019).
[7] A. Arenas, A. Díaz-Guilera, J. Kurths, Y. Moreno, and C. Zhou, "Synchronization in complex networks," Phys. Rep. **469**, 93 (2008).
[8] C. del Genio, J. Gómez-Gardeñes, I. Bonamassa, and S. Boccaletti, "Synchronization in networks with multiple action layers," Sci. Adv. **2**, e1601679 (2016).
[9] Y. Zhang, G. Hu, H. A. Cerdeira, S. Chen, T. Braun, and Y. Yao, "Partial synchronization and spontaneous spatial ordering in coupled chaotic systems," Phys. Rev. E **63**, 026211 (2001).
[10] P. Ji, T. K. D. Peron, F. A. Rodrigues, and J. Kurths, "Analysis of cluster explosive synchronization in complex networks," Phys. Rev. E **90**, 062810 (2014).
[11] R. Lauter, A. Mitra, and F. Marquardt, "From Kardar-Parisi-Zhang scaling to explosive desynchronization in arrays of limit-cycle oscillators," Phys. Rev. E **96**, 012220 (2017).
[12] Y. Kuramoto and D. Battogtokh, "Coexistence of coherence and incoherence in nonlocally coupled phase oscillators," Nonlinear Phenom. Complex Syst. **5**, 380–385 (2002).
[13] L. Schmidt, K. Schönleber, K. Krischer, and V. García-Morales, "Coexistence of synchrony and incoherence in oscillatory media under nonlinear global coupling," Chaos **24**, 013102 (2014).
[14] L. Schmidt and K. Krischer, "Clustering as a prerequisite for chimera states in globally coupled systems," Phys. Rev. Lett. **114**, 034101 (2015).
[15] A. Mishra, C. Hens, M. Bose, P. K. Roy, and S. K. Dana, "Chimeralike states in a network of oscillators under attractive and repulsive global coupling," Phys. Rev. E **92**, 062920 (2015).

[16]D. Dudkowski, Y. Maistrenko, and T. Kapitaniak, "Different types of chimera states: An interplay between spatial and dynamical chaos," Phys. Rev. E **90**, 032920 (2014).
[17]C. Castellano, S. Fortunato, and V. Loreto, "Statistical physics of social dynamics," Rev. Mod. Phys. **81**, 591 (2009).
[18]R. Pastor-Satorras, C. Castellano, P. Van Mieghem, and A. Vespignani, "Epidemic processes in complex networks," Rev. Mod. Phys. **87**, 925 (2015).
[19]Y.-Y. Liu, J.-J. Slotine, and A.-L. Barabási, "Controllability of complex networks," Nature **473**, 167 (2011).
[20]L. M. Pecora and T. L. Carroll, "Master stability functions for synchronized coupled systems," Phys. Rev. Lett. **80**, 2109 (1998).
[21]S. Boccaletti, G. Bianconi, R. Criado, C. I. Del Genio, J. Gómez-Gardenes, M. Romance, I. Sendina-Nadal, Z. Wang, and M. Zanin, "The structure and dynamics of multilayer networks," Phys. Rep. **544**, 1 (2014).
[22]J. I. Mondragon, J. Raul, and G. Bianconi, "Multilink communities of multiplex networks," PLoS One **13**, e0193821 (2018).
[23]S. Boccaletti, R. Criado, M. Romance, and J. J. Torres, "Introduction to focus issue: Complex dynamics in networks, multilayered structures and systems," Chaos **26**, 065101 (2016).
[24]I. Leyva, R. Sevilla-Escoboza, I. Sendina-Nadal, R. Gutierrez, J. Buldu, and S. Boccaletti, "Inter-layer synchronization in nonidentical multi-layer networks," Sci. Rep. **7**, 1–9 (2017).
[25]S. Ghosh, A. Zakharova, and S. Jalan, "Non-identical multiplexing promotes chimera states," Chaos Solitons Fractals **106**, 56 (2018).
[26]O. E. Rössler, "Continuous chaos—Four prototype equations," Ann. N. Y. Acad. Sci. **316**, 376 (1979).
[27]P. Louodop, S. Saha, R. Tchitnga, P. Muruganandam, S. K. Dana, and H. A. Cerdeira, "Coherent motion of chaotic attractors," Phys. Rev. E **96**, 042210 (2017).
[28]W. Zou, D. Senthilkumar, R. Nagao, I. Z. Kiss, Y. Tang, A. Koseska, J. Duan, and J. Kurths, "Restoration of rhythmicity in diffusively coupled dynamical networks," Nat. Commun. **6**, 1–9 (2015).
[29]D. Ghosh, T. Banerjee, and J. Kurths, "Revival of oscillation from mean-field-induced death: Theory and experiment," Phys. Rev. E **92**, 052908 (2015).
[30]R. Karnatak, R. Ramaswamy, and A. Prasad, "Amplitude death in the absence of time delays in identical coupled oscillators," Phys. Rev. E **76**, 035201 (2007).
[31]S. Cafieri, L. Cellier, F. Messine, and R. Omheni, "Combination of optimal control approaches for aircraft conflict avoidance via velocity regulation," Optim. Control Appl. Methods **39**, 181 (2018).
[32]H.-B. Chen, Y.-T. Sun, J. Gao, C. Xu, and Z.-G. Zheng, "Order parameter analysis of synchronization transitions on star networks," Front. Phys. **12**, 120504 (2017).
[33]H. Hong and M. Choi, "Phase synchronization and noise-induced resonance in systems of coupled oscillators," Phys. Rev. E **62**, 6462 (2000).
[34]G. Hu, Y. Zhang, H. A. Cerdeira, and S. Chen, "From low-dimensional synchronous chaos to high-dimensional desynchronous spatiotemporal chaos in coupled systems," Phys. Rev. Lett. **85**, 3377 (2000).
[35]Y. Maistrenko, O. Popovych, O. Burylko, and P. A. Tass, "Mechanism of desynchronization in the finite-dimensional Kuramoto model," Phys. Rev. Lett. **93**, 084102 (2004).
[36]C. Allefeld, M. Müller, and J. Kurths, "Eigenvalue decomposition as a generalized synchronization cluster analysis," Int. J. Bifurc. Chaos **17**, 3493 (2007).
[37]J. Singha, V. Tchuyang, P. Louodop, R. Tchitnga, H. A. Cerdeira, and N. Gupte, "Spatial splay states in coupled map lattices and Josephson junction arrays," Ind. Acad. Sci. **1**, 195–203 (2017).
[38]S. Nichols and K. Wiesenfeld, "Ubiquitous neutral stability of splay-phase states," Phys. Rev. A **45**, 8430 (1992).
[39]H. Fujisaka and T. Yamada, "Stability theory of synchronized motion in coupled-oscillator systems," Prog. Theor. Phys. **69**, 32 (1983).
[40]L. M. Pecora and T. L. Carroll, "Synchronization in chaotic systems," Phys. Rev. Lett. **64**, 821 (1990).
[41]K. Pearson, "Notes on the history of correlation," Biometrika **13**, 25 (1920).
[42]H. Hong and S. H. Strogatz, "Mean-field behavior in coupled oscillators with attractive and repulsive interactions," Phys. Rev. E **85**, 056210 (2012).
[43]K. Sathiyadevi, V. Chandrasekar, D. Senthilkumar, and M. Lakshmanan, "Distinct collective states due to trade-off between attractive and repulsive couplings," Phys. Rev. E **97**, 032207 (2018).
[44]J. F. Denijs and M. Lindner, "Transmission for converting rotary motion into linear motion," U.S. patent 5,690,567 (1997).
[45]A. Farshidianfar and A. Saghafi, "Identification and control of chaos in nonlinear gear dynamic systems using Melnikov analysis," Phys. Lett. A **378**, 3457–3463 (2014).
[46]F. M. Kakmeni, S. Bowong, D. Senthikumar, and J. Kurths, "Practical time-delay synchronization of a periodically modulated self-excited oscillators with uncertainties," Chaos **20**, 043121 (2010).
[47]S. Majhi, M. Perc, and D. Ghosh, "Chimera states in uncoupled neurons induced by a multilayer structure," Sci. Rep. **6**, 39033 (2016).
[48]L. Tang, X. Wu, J. Lü, J.-A. Lu, and R. M. D'Souza, "Master stability functions for complete, intralayer, and interlayer synchronization in multiplex networks of coupled rössler oscillators," Phys. Rev. E **99**, 012304 (2019).
[49]L. Huang, Q. Chen, Y.-C. Lai, and L. M. Pecora, "Generic behavior of master-stability functions in coupled nonlinear dynamical systems," Phys. Rev. E **80**, 036204 (2009).
[50]Based on Ref. 27, a system is considered as jerk if the flow can be rewritten as a third order differential equation in a single scalar variable. For an isolated system, the jerk system can be defined as: $\dddot{x}_2 = \alpha\left(-\beta\left(-\dot{x}_1 + \dot{x}_2 - \gamma\ddot{x}_1 + \frac{\gamma}{\alpha}\ddot{x}_2\right) + \ddot{x}_1\right)$, where $\ddot{x}_1 = I'(x_2)\dot{x}_2$ and $\dddot{x}_1 = I''(x_2)\dot{x}_2^2 + I'(x_2)\ddot{x}_2$. Then, $\dddot{x}_1$ is called the jerk function.